Effects of source and substrate temperatures on the properties of ITO/CuPc/C_{60} heterostructure prepared by physical vapor deposition

Kuan-Cheng Chiu[a],*, Liu-Ting Juey[a], Chih-Feng Su[a], Shiow-Jing Tang[a], Ming-Nan Jong[a], Sheng-Shin Wang[a], Jyh-Shyang Wang[a], Chu-Shou Yang[b], Wu-Ching Chou[b]

[a]*Department of Physics and R & D Center for Membrane Technology, Chung Yuan Christian University, Chung-Li 32023, Taiwan, ROC*
[b]*Department of Electrophysics, National Chiao Tung University, Hsin-Chu 30010, Taiwan, ROC*

Available online 7 November 2007

Abstract

Small-molecule organic photovoltaic (OPV) cells with a heterostructure of indium tin oxide (ITO)/copper phthalocyanine (CuPc)/C_{60}/ Ag were fabricated by physical vapor deposition at different source temperatures T_{sou} and substrate temperatures T_{sub}. The physical properties of these as-deposited organic thin films including surface morphology, structural information, and electrical and optical properties were measured (in layer-by-layer sequence) by atomic force microscopy, X-ray diffraction, current–voltage characteristics, and electronic absorption spectra. At first, the effects of different deposition conditions (T_{sou} and T_{sub}) on growth rate and film thickness of these organic thin films were examined. Then, the interface properties of ITO/CuPc and CuPc/C_{60} were studied with respect to T_{sub}. Short-circuit current density J_{sc} and open-circuit voltage V_{oc} for this ITO/CuPc/C_{60}/Ag heterostructure under illumination were performed, and the spectral response of J_{sc} was analyzed. Finally, the T_{sub}-dependence of the physical properties of the as-deposited organic films and of the performance of the as-fabricated OPV cells were discussed.

1. Introduction

With the awareness that fossil fuels are being depleted, solar cells based on photovoltaic (PV) effect, which directly convert incident sunlight into electricity, will ultimately play an important role in the world's energy market. Currently, Si wafer-based p–n junction PV cells and GaAs-based heterostructure PV cells are commercially available and dominate this market. These PV cells with multilayer structures are adopted, because the incident sunlight can be splittingly absorbed by various layers of different energy gaps, and thus the sunlight is converted into electricity more efficiently. To fabricate multilayer structures, thin film deposition technologies are employed, and the materials deposited include amorphous silicon, polycrystal-line silicon, cadmium telluride, copper indium selenide/ sulfide, polymers, small organic molecules, etc. [1]. Among them, PV cells made from organic semiconductor materials (small-molecule organic compounds or polymers) possess low fabrication cost, easy processability, light weight and mechanical flexibility, and thus promise to open up new markets for solar energy [2,3]. However, the development of large-scale applications of organic photovoltaic (OPV) cells is still limited by their low energy conversion efficiency as well as by the device stability and degradation problems.

In multilayer OPV cells, after light absorption in the active absorbing parts, strongly bound excitons are generated. These bound excitons then diffuse and dissociate into free charge carriers by interaction with heterostructure interfaces, impurities or defects, and the free electrons and holes are collected by the respective electrodes. The overall performance of OPV cells is sensitively dependent on light absorption, exciton diffusion

---

*Corresponding author. Tel.: +886 32653213; fax: +886 32653299.
E-mail address: kcchiu@phys.cycu.edu.tw (K.-C. Chiu).

and dissociation behaviors, and free-charges transport and collection ability. Therefore, the choice of materials [3–11], the design of cell structures [10–16] and the deposition conditions [17,18] all play important roles in determining the power conversion efficiency (PCE) of OPV cells.

To investigate the influences of deposition conditions on PCE of OPV cells, in this paper, small-molecule OPV cells based on a heterostructure of indium tin oxide (ITO)/ copper phthalocyanine (CuPc)/C_{60}/Ag were fabricated by physical vapor deposition (PVD) at various source temperatures T_{sou} and substrate temperatures T_{sub}. From a crystal grower's point of view, during PVD processes, both T_{sou} and T_{sub} markedly affect the qualities of the as-deposited films, and these effects were clearly exhibited by our earlier experimental results on C_{60} polycrystalline films [19,20] and tris(8-hydroxyquinoline)aluminum (Alq$_3$) amorphous layers [21,22]. To extend these experimental findings from a single layer structure to a sophisticated and complicated optoelectronic heterostructure, the effects of T_{sou} and T_{sub} on the performance of OPV cells with a heterostructure of ITO/CuPc/C_{60}/Ag prepared by PVD were studied.

2. Experimental procedure

The samples were prepared by PVD in a thermal evaporation chamber with a base pressure of about 2×10^{-5} Torr. ITO conducting glass with sheet resistance of $13 \pm 2\,\Omega$/square was used as a substrate. The distance between source crucibles and ITO substrate was about 16 cm. The values of T_{sou} were varied from 330 to 360 °C for CuPc and 370 to 460 °C for C_{60}, and T_{sub} was fixed at 30 and 90 °C, respectively. Commercially available source powders of CuPc (with a purity of 98%) and C_{60} (99.5%) were used as received and were loaded separately in boron nitride crucibles. Before reaching the setting T_{sou}, the source powder was kept at 70, 180 and 280 °C in sequence for an additional 20 min heat treatment, in order to evaporate any possible moisture or impurities involved during the handling of the source powders into the system. When T_{sou} and T_{sub} attained the setting values, the shutter in between the source crucibles and substrate was removed to allow vacuum deposition. The deposition rate was maintained at 0.3–0.5 Å/s. After the thickness of the CuPc film reached the required value, the heating system was turned off and cooled down naturally; then, the deposition process was repeated again for the C_{60} thin film. Finally, the sample was removed out of the vacuum chamber, and the Ag thin film with an active area $A = 0.03$ cm^2 was ion-sputtered through a mask on top of ITO/CuPc/C_{60} as the cathode.

The dark and illuminated current density–voltage (J–V) characteristics were measured in dynamic vacuum conditions to prevent the samples from photo-oxidation. To measure the illuminated J–V curves, the sample was kept under weak white light illumination (with a power of 0.85 ± 0.05 mW/cm^2) from a simple incandescent lamp of 60 W. The intensity of light was measured separately using a calibrated Si photodiode placed at the same position as the sample. For electronic absorption studies, a 150 W tungsten–halogen lamp with a scanning monochromator was used as the light source. The photocurrent spectrum of the sample at short-circuit was measured and normalized with respect to the spectral intensity of incident light.

3. Results and discussion

During PVD processes in a vacuum chamber, T_{sou} determines the vapor pressure of the source powder and plays an important role in determining the growth rate of the as-deposited film. Fig. 1 depicts a typical time-dependence of the growth rate for a C_{60} thin film with $T_{sub} = 30$ °C and with a fixed amount of source powder. At higher T_{sou}, the growth rate decays quickly. In addition, if T_{sou} is too high, the organic source compounds tend to decompose easily. Therefore, T_{sou} associated with a reasonably low growth rate is usually adopted in order to have a better control of film thickness.

Fig. 2 presents the typical atomic force microscopic (AFM) pictures of fine-grain surface morphology for ITO/ CuPc/C_{60} deposited at $T_{sub} = 30$ and 90 °C, respectively. For solid films made from small-molecule organic compounds, the dominant force between organic molecules is the weak van der Waals force. Thus, the dependence of surface morphology on T_{sub} is expected to be strong. As shown in Fig. 2, with increasing T_{sub} from 30 up to 90 °C, to enhance the surface diffusion energy of the adhered organic molecules, the average surface roughness observed in C_{60} interface then decreases from 8.8 ± 0.4 down to 2.7 ± 0.3 nm. The strong T_{sub}-dependence of surface morphology in molecular solids is in good agreement with those results obtained in CuPc:C_{60} (1:1) blend films with T_{sub} varied from 30 to 145 °C [18]. For $T_{sub} \geqslant 150$ °C, formation of line fiber was observed in the surface of
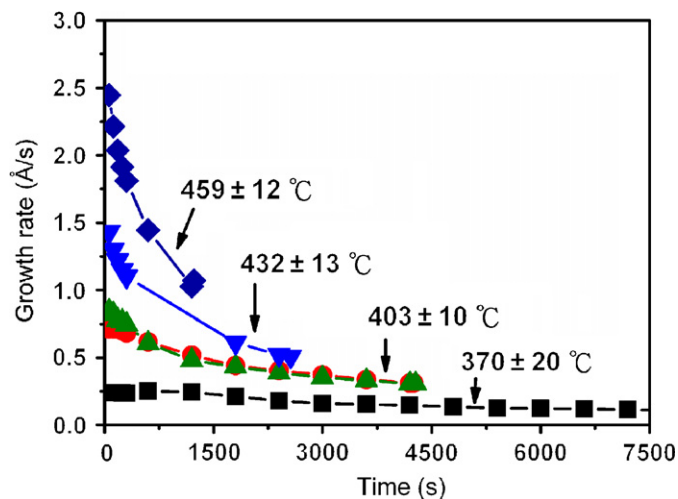

Fig. 1. Time dependence of growth rate at various T_{sou} for C_{60} thin film with a fixed amount of source powder.
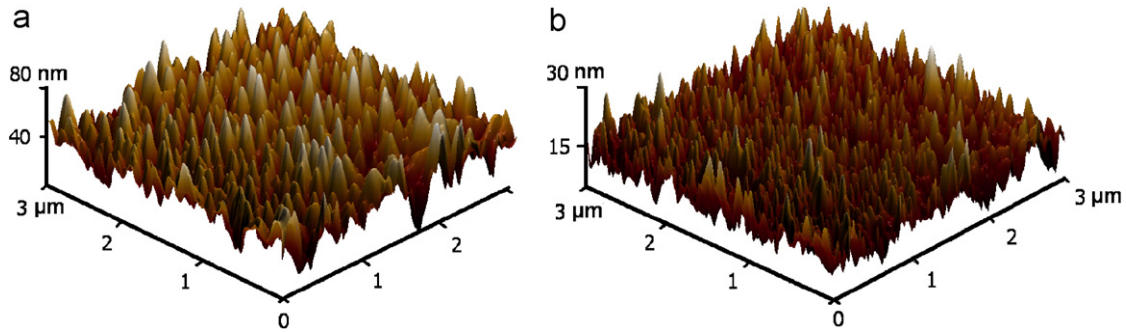
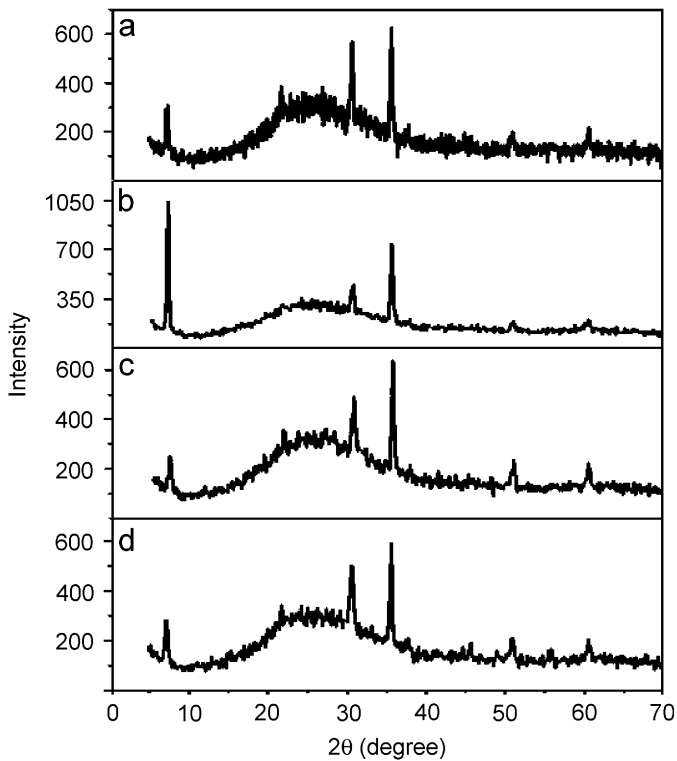Fig. 2. AFM pictures for ITO/CuPc/C$_{60}$ deposited at T_{sub} = (a) 30 °C and (b) 90 °C.

Fig. 3. XRD patterns for ITO/CuPc films deposited at T_{sub} = (a) 30 °C and (b) 90 °C, and for ITO/CuPc/C$_{60}$ films deposited at T_{sub} = (c) 30 °C and (d) 90 °C, respectively. Note the adjustment of the vertical scale in (b).
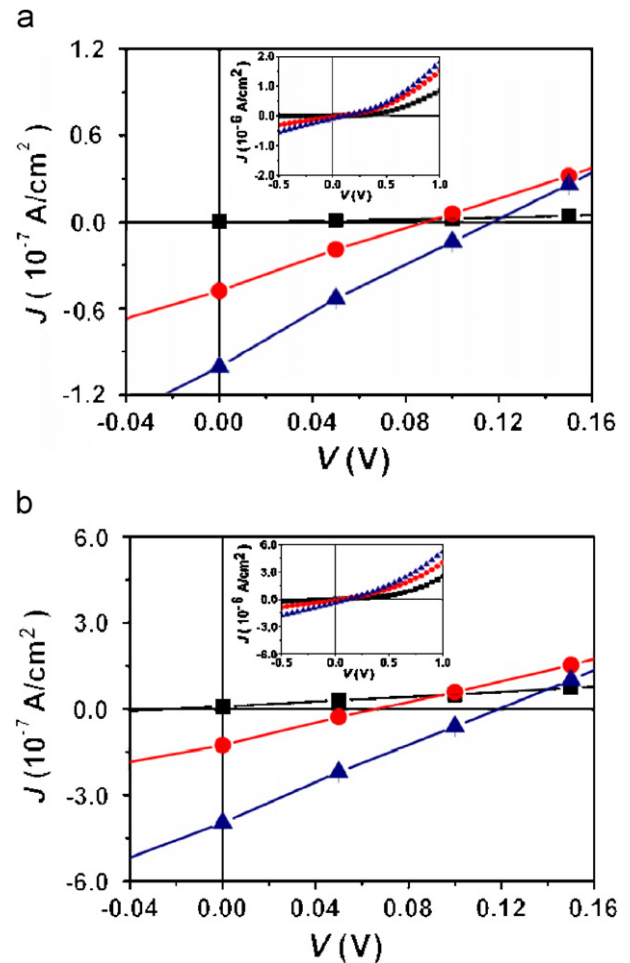

Fig. 4. The dark and illuminated (with two different power levels) J–V characteristics of the ITO/CuPc/C$_{60}$/Ag devices deposited at T_{sub} = (a) 30 °C and (b) 90 °C.

CuPc films [17]. Hence, in this work, T_{sub} = 90 °C is taken to investigate the high-T_{sub} effects.

Fig. 3 depicts the XRD patterns for ITO/CuPc and ITO/CuPc/C$_{60}$ films deposited at T_{sub} = 30 and 90 °C, respectively. At T_{sub} = 30 °C, the deposited organic CuPc thin films on top of ITO should exhibit amorphous character, and the two strong peaks observed at 2θ = 30.6° and 35.5° correspond to (2 2 2) and (4 0 0) planes of ITO films. It is noted that CuPc undergoes a solid–solid phase transition from α-phase (orthohomic) to β-phase (monoclinic) at around 200–240 °C [13,17]. In the present work, as shown in Fig. 3(a) for T_{sub} = 30 °C, the characteristic weak peak at 2θ = 7.0° is occasionally observed, which corresponds to the (2 0 0) plane of α-CuPc phase; while for T_{sub} = 90 °C as shown in Fig. 3(b), this (2 0 0) peak is dominant, indicating

that the crystalline α-CuPc phase is prevailing. However, after deposition of a thin amorphous C$_{60}$ film of 150 nm, the prevailing crystalline α-CuPc phase is reduced as depicted in Figs. 3(c) and (d). For molecular α-CuPc film, the impingement of C$_{60}$ molecules on the interface may strongly alter its film's crystallinity.

Fig. 4 shows the dark and illuminated J–V characteristics of two typical ITO/CuPc/C$_{60}$/Ag devices fabricated at T_{sub} = 30 and 90 °C, respectively. For dark J–V curves, in

view of the very thin layer thickness of the samples, a space charge limited current (SCLC) can dominate the transport behaviors [23,24]. Thus, J–V behavior follows a simple power law as $J \propto V^\alpha$, where $\alpha = 1.5$ for the case of negligible energy loss of the carriers and known as Child–Langmuir law, and $\alpha = 2.0$ for the case of constant mobility and known as Mott–Gurney law. From a $\log J$ versus $\log V$ plot, two distinct linear regions are shown in our data. By least-square fitting, for low biases ($V = 0$–0.4 V) as listed in Table 1, $\alpha_L = 1.2 \pm 0.1$ indicates that the transport behavior is in a mixed regime governed by ohmic law ($\alpha = 1$) and Child–Langmuir law ($\alpha = 1.5$). However, as the electric field increases, a transition was observed from an ohmic law to a Mott–Gurney law, and during the transition a large value of $\alpha = 8$ was obtained, which may be caused by the onset of carrier injection and trap filling [24]. Based on this finding, the scattered values of α_H for high biases ($V = 0.5$–1.0 V) ranging from 2.1 to 4.7 (as listed in Table 1) indicate that the electric fields applied to these samples are near the onset of the above-mentioned transition.

In addition, the dark current densities measured in our OPV cells are rather small, which resulted by the exposure to air/oxygen before deposition of Ag-electrode. Because of the diffusion of O_2 into C_{60} solids, the resistivity of C_{60} film increases several orders of magnitude [25–27]. Accordingly, the dark current densities of these OPV cells are greatly reduced.

The J–V characteristics of ITO/CuPc/C_{60}/Ag devices under white light illumination clearly demonstrate the PV effect, as shown in Fig. 4 with two different optical intensities (about 0.28 ± 0.05 and 0.85 ± 0.05 mW/cm^2). The experimental values of short-circuit current density J_{sc}, open-circuit voltage V_{oc}, and fill factor FF determined for these OPV cells fabricated at $T_{sub} = 30$ and 90 °C are listed in Table 1. Because of low incident optical intensity and large series resistance, the values of J_{sc} observed in this work are much smaller as compared to the results obtained by using a simulated AM1.5G illumination of 75–100 mW/cm^2 [8,9,18]. However, with respect to T_{sub}-dependence, one can see that OPV cells fabricated at $T_{sub} = 90$ °C can deliver more power output (about a factor of 5) than those fabricated at $T_{sub} = 30$ °C.

To investigate the electronic absorption and charge-carrier collection ability, a spectral response of normalized

short-circuit current I_{sc} for OPV devices was performed. As shown in Fig. 5(a), the two curves were measured on the same device but with a time separation of 2 h in dynamic vacuum conditions. Clearly, there are three main absorption peaks at wavelengths of 703 ± 2, 614 ± 3, and 463 ± 2 nm, which are in good agreement with the published results [16]. In order to understand the origin of these peaks, the absorption spectra of CuPc (with thickness of 120 nm) and C_{60} (with thickness of 150 nm) amorphous films were examined as shown in Fig. 5(b), which are also similar to the published data [10,15,16,18]. From a comparison of Figs. 5(a) and (b), the two peaks of 703 and 614 nm are associated with the CuPc film (with threshold absorption energies around 1.58 and 1.87 eV) while the third one of 463 nm can be attributed to the C_{60} film (with threshold absorption energy around 2.38 eV). Thus, the photon-generated excitons either at the CuPc thin layer or at C_{60} thin film can be effectively separated and collected as short-circuit current as revealed in Fig. 5(a). In discussing optical absorption of organic molecular solids, the energy difference between the highest occupied molecular orbits (HOMO) and the lowest unoccupied molecular orbits (LUMO) is usually referred. However, in molecular solids, many molecules are brought

Table 1
Comparison of PV and SCLC parameters for ITO/CuPc/C60/Ag devices fabricated at various T_{sub} and CuPc/C_{60} film thicknesses

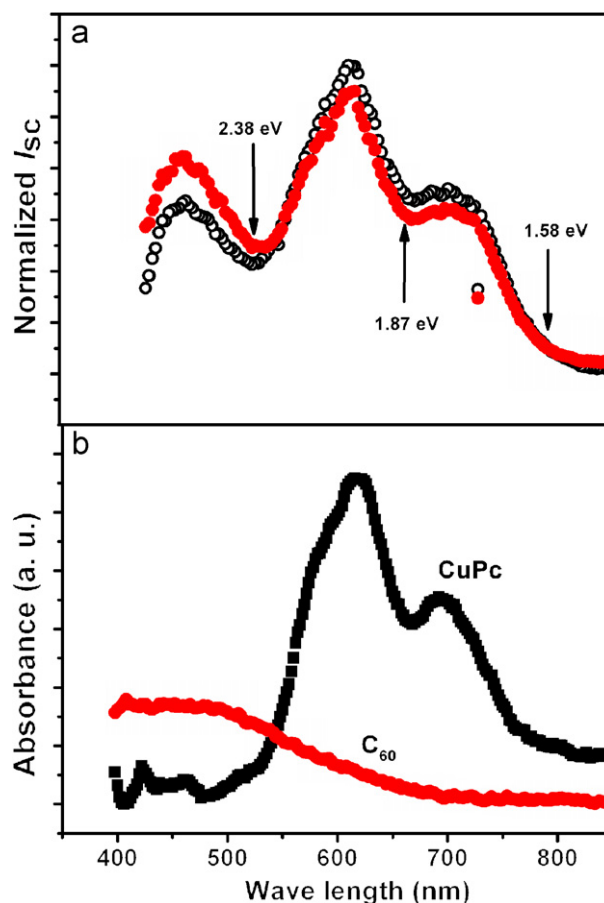| T_{sub} (°C)	CuPc (nm)	C_{60} (nm)	J_{sc} (nA/cm^2)	V_{oc} (V)	P_m (nW/cm^2)	FF	α_L/α_H
30	200	150	100	0.12	2.8	0.24	1.5/2.8
30	200	150	52	0.19	2.3	0.23	1.2/2.1
30	120	150	27	0.22	1.4	0.24	1.1/2.1
90	200	150	430	0.12	12.3	0.23	1.1/2.2
90	120	150	205	0.23	14.0	0.30	1.2/4.7

Fig. 5. (a) Spectral response of the normalized I_{sc} for the ITO/CuPc/C_{60}/Ag device and (b) absorption spectra of CuPc (thickness of 120 nm) and C_{60} (thickness of 150 nm) thin amorphous films.

close together, so that the split energy levels of HOMO and LUMO form continuous energy bands with a small energy bandwidth due to the weak van der Waals force. From spectral broadening, as shown in Fig. 5(b), the energy bandwidths for CuPc amorphous films are estimated to be approximately 0.11–0.21 eV, while the bandwidths for C_{60} amorphous films are much wider and difficult to be estimated in this way.

The above experimental results reveal that the deposition conditions, especially for T_{sou} and T_{sub}, profoundly affect the physical properties of the as-deposited organic molecular films as well as the performance of the as-fabricated OPV cells. With the appropriate choice of T_{sou} and by slightly increasing T_{sub}, the adhered organic molecules on the growing interface gain more surface diffusion energy and the as-deposited layer then possesses flatter surface morphology and more compact structure. A longer exciton diffusion length and a higher value of charge-carrier mobility may result due to less scattering and, accordingly, J_{sc} and PCE of the OPV cells increase. However, further increasing T_{sub} may lead to a complex interplay of surface mobility and re-evaporation of the adhered molecules [19,20]. The formation of line fibers observed in CuPc films for $T_{sub} \geqslant 150\,^{\circ}C$ [17] can additionally set an upper limit of T_{sub} for obtaining a smooth amorphous CuPc film, and the physical properties of CuPc films deposited at $T_{sub} \geqslant 150\,^{\circ}C$ and the performance of OPV devices fabricated from these films remain to be further investigated.

4. Summary

Small-molecule OPV cells with a heterostructure of ITO/CuPc/C_{60}/Ag were fabricated by PVD at various T_{sou} and T_{sub}. To have a better control of film thickness and to prevent organic compounds from thermal decomposition, T_{sou} (in between 330 and 360 °C for CuPc and 370 and 460 °C for C_{60}) associated with a reasonably low growth rate was adopted. With increasing T_{sub} from 30 up to 90 °C, the average surface roughness in ITO/CuPc/C_{60} interface decreases from 8.8 down to 2.7 nm. From a fit of dark J–V curves, two distinct linear regions were shown and discussed. In addition, the measured values of J_{sc} and V_{oc} for these devices under illumination reveal that the OPV cells fabricated at $T_{sub} = 90\,^{\circ}C$ were found to deliver more power output than those fabricated at $T_{sub} = 30\,^{\circ}C$. This strong T_{sub}-dependence observed in this work suggests that the organic molecular film deposited at a higher T_{sub} possesses a flatter surface morphology and a more compact structure, and, accordingly, PCE of the as-fabricated OPV cells increases.

References

[1] Y. Hamakawa (Ed.), Thin-Film Solar Cells: Next Generation Photovoltaics and its Application, Springer, Berlin, 2004.
[2] H. Spanggaard, F.C. Krebs, Sol. Energy Mater. Sol. Cells 83 (2004) 125.
[3] M.C. Scharber, D. Muhlbacher, M. Koppe, P. Denk, C. Waldauf, A.J. Heeger, C.J. Brabec, Adv. Mater. 18 (2006) 789.
[4] C.W. Tang, Appl. Phys. Lett. 48 (1986) 183.
[5] W. Gao, A. Kahn, Appl. Phys. Lett. 82 (2003) 4815.
[6] C.W. Chu, V. Shrotriya, G. Li, Y. Yang, Appl. Phys. Lett. 88 (2006) 153504.
[7] O.V. Molodtsova, M. Knupfer, J. Appl. Phys. 99 (2006) 53704.
[8] M.L. Wang, Q.L. Song, H.R. Wu, B.F. Ding, X.D. Gao, X.Y. Sun, X.M. Ding, X.Y. Hou, Org. Electron. 8 (2007) 445.
[9] H. Derouiche, V. Djara, Sol. Energy Mater. Sol. Cells 91 (2007) 1163.
[10] T. Stubinger, W. Brutting, J. Appl. Phys. 90 (2001) 3632.
[11] Z.R. Hong, Z.H. Huang, X.T. Zeng, Chem. Phys. Lett. 425 (2006) 62.
[12] P. Peumans, V. Bulovic, S.R. Forrest, Appl. Phys. Lett. 76 (2000) 2650.
[13] S.M. Schultes, P. Sullivan, S. Heutz, B.M. Sanderson, T.S. Jones, Mater. Sci. Eng. C25 (2005) 858.
[14] K. Triyana, T. Yasuda, K. Fujita, T. Tsutsui, Thin Solid Films 477 (2005) 198.
[15] M.Y. Chan, C.S. Lee, S.L. Lai, M.K. Fung, F.L. Wong, H.Y. Sun, K.M. Lau, S.T. Lee, J. Appl. Phys. 100 (2006) 94506.
[16] T. Osasa, S. Yamamoto, M. Matsumura, Jpn. J. Appl. Phys. 45 (2006) 3762.
[17] J.E.S. Kim, E. Lim, K. Lee, D. Cha, B. Friedman, Appl. Surf. Sci. 205 (2003) 274.
[18] M. Vogel, J. Strotmann, B. Johnev, M.C. Lux-Steiner, K. Fostiropoulos, Thin Solid Films 511 (2006) 367.
[19] R.S. Chen, Y.J. Lin, Y.C. Su, K.C Chiu, Thin Solid Films 396 (2001) 103.
[20] W.R. Cheng, S.J. Tang, Y.C. Su, Y.J. Lin, K.C. Chiu, J. Crystal Growth 247 (2003) 401.
[21] J.M. Chung, Y.Z. Luo, Z.A. Jian, M.C. Kuo, C.S. Yang, W.C. Chou, K.C. Chiu, Jpn. J. Appl. Phys. Part I 43 (2004) 1631.
[22] Z.A. Jian, et al., J. Appl. Phys. 101 (2007) 123708.
[23] K. Fess, Advanced Theory of Semiconductor Devices, Prentice-Hall, Englewood Cliffs, NJ, 1998.
[24] M. Kiy, P. Losio, I. Biaggio, M. Koehler, A. Tapponnier, P. Gunter, Appl. Phys. Lett. 80 (2002) 1198.
[25] C.M. Yang, J.L. Liao, K.C. Chiu, J. Appl. Phys. 96 (2004) 1934.
[26] B. Brousse, B. Ratier, A. Moliton, Synth. Met. 147 (2004) 293.
[27] M. Rusu, J. Strotmann, M. Vogel, M.Ch. Lux-Steiner, K. Fostiropoulos, Appl. Phys. Lett. 90 (2007) 153511.